20th Australasian Fluid Mechanics Conference
Perth, Australia
5-8 December 2016

Assessing the relationship between bed shear stress estimates and observations of sediment resuspension in the ocean

C.E. Bluteau, S.-L. Smith, G.N. Ivey, T.L. Schlosser and N.L. Jones

[1]School of Civil, Environmental and Mining Engineering & The Oceans Institute
The University of Western Australia, Western Australia 6009, Australia

Abstract

We present observations from a three week field programme on the Tasman Eastern Continental Shelf designed to determine the mechanisms responsible for sediment resuspension when tidally-forced internal waves impinge on the shelf. Using a bottom lander on the seafloor at the 190 m isobath, we measured sediment concentrations, velocities, and turbulent stresses near the seabed. The bed shear stress estimated using the quadratic drag law had the highest correlation with the observed sediment concentrations, but were always much higher than the critical shear stress required to initiate sediment motion. Bed shear stresses determined from the turbulence measurements were more reasonable in magnitude, but unresolved questions remain. Our ultimate goal is to improve predictions of near-bed shear stresses, and sediment re-suspension in these complex flows.

Introduction

Tidally-driven internal waves are energetic, ubiquitous, and persistent oceanic phenomena that contribute to and can even dominate the resuspension and transport of sediment on continental slopes and shelves [4]. Recent field, laboratory and numerical studies have demonstrated that nonlinear internal waves can significantly suspend and transport sediment as they propagate [5], shoal [3] or break [12]. Despite the complexity of the near-bed turbulent motions that lead to resuspension, modelling studies continue to employ empirical parameterisations based on simple steady flows to estimate the bottom shear stress τ_w [11] and hence sediment resuspension. Here, we use field measurements to examine the near-bed turbulence dynamics and resulting sediment suspension in order to assess different methods of estimating bottom shear stresses τ_w, which we then compare with observations of suspended sediment concentrations.

Predicting bed shear stress

We assess three methods for estimating τ_w. The first, and simplest method, is the quadratic law:

$$\tau_{wD} = \rho C_d U^2 \tag{1}$$

where ρ is the density of water, C_d is the drag coefficient dependent on the mean velocity U and roughness of the boundary. The second method to determine τ_w relies on its relationship with the shear velocity u_τ:

$$\tau_{wI} = \rho u_\tau^2. \tag{2}$$

The shear velocity u_τ here can be determined from [6]:

$$u_\tau = (\varepsilon \kappa z)^{1/3} \tag{3}$$

where the rate of turbulent kinetic energy dissipation ε is measured at a height z from the bottom. We denote this second method as the inertial dissipation (ID) method. Both of these methods for obtaining u_τ assume the mean velocity profile is logarithmic and that the flow is un-stratified, steady and unidirectional. The turbulence shear production term of the turbulent kinetic energy equation must also balance ε. The third method we assess is a modified version of the turbulent kinetic energy method [1, 6]:

$$\tau_{wT} = \rho C_t \overline{w'w'} \tag{4}$$

that relies on the turbulent vertical velocity w'. We set the constant C_t to 0.9 [6] and the overbar denotes a temporal average. This third method, which we denote as the TKE method, is expected to fair better in more complex flows [1] or when the measurements are outside the log-law region [6].

Field measurements

We undertook an internal wave and sediment resuspension study on the Tasman Eastern continental Shelf (TES) for 3 weeks in February 2015. During this study, a bottom lander was deployed at the shelf-break in 185 m of water (figure 1). Thermistors were attached to the lander and to a 20-m long mooring line extending upwards from it, providing high vertical resolution (0.5 m) temperature measurements near the seabed (table 1). We estimated the background density stratification N from these thermistors and a conductivity sensor on the lander. Other instrumentation on the lander included: a 1200 kHz acoustic-Doppler current profiler (RDI, Teledyne) measuring mean velocities over the bottom 13 m, an acoustic suspended sediment profiler (AQUAscat 1000R, AquaTec), and an optical backscatter sensor at 1.2m ASB (OBS; FLNTUSB, WetLabs).

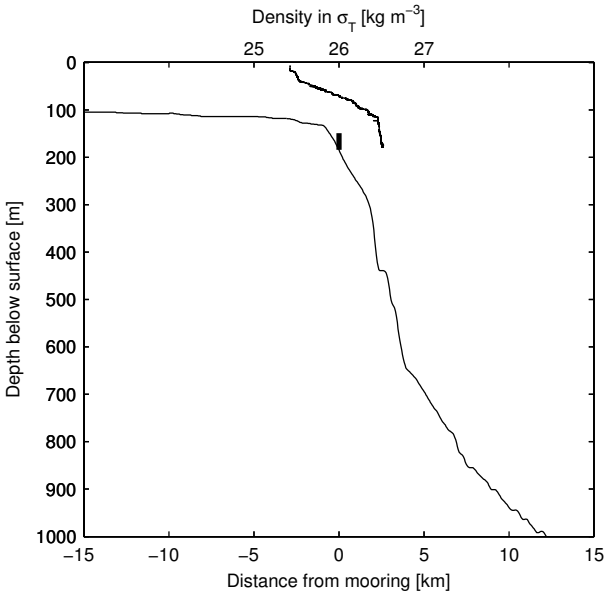

Figure 1: Cross-shelf topography with the bottom lander's location and the time-averaged vertical density profile from the nearby mooring.

Two acoustic-Doppler velocimeters (ADV; Vector, Nortek-AS) were also mounted on the lander to measure turbulent velocities at 64 Hz at 0.4 and 1.4 m ASB. The rate of turbulent kinetic energy dissipation ε was estimated from the inertial subrange of the ADVs' velocity spectra [2], and u_τ then estimated from equation 3. We estimated these spectra from 8.5 min (512 s) long segments, that overlapped by 50%, and used these same segments to estimate $\overline{w'w'}$. From these $\overline{w'w'}$ and ε estimates, we used equation 2 and 4 to estimate τ_{wT} and τ_{wI}.

Table 1: Instruments' sampling programme for the bottom lander located in 190 m of water (148.6314°E, 41.3865°S)

Instrument	Height above seabed (m ASB)	Sampling details
Thermistors	0.3b, 0.8c, 1.3d, 3.1b, 3.7b, 4.6b, 5.7b, 6.7b, 8.2b, 10.2b, 12.2b, 14.3b, 16.3b, 20.4a	a=SBE39 with pressure at 10 s, b=SBE56 at 2Hz, c=SBE37 at 20 s
ADVs	0.4 with pressure, 1.4 with FP07	64 Hz
ADCP	0.25 m bins from 1 to 12 m ASB	Recording each 1 s ping (mode 12)
OBS	1.2	3 samples at 1 Hz every min
AquaScat	1 cm bins from 0 to 1.1 m ASB	Pinged at 64 Hz but stored at 4Hz. 1 MHz, 2 MHz, 4 MHz, and 0.5 MHz transducers.

We also deployed a through-water column mooring about 300 m away from the lander site. The mooring was equipped with 14 thermistors and one conductivity-temperature sensor all sampling at 10 s intervals. A 150 kHz acoustic-Doppler current profiler (RDI, Teledyne) recorded velocities in 2 m vertical bins over most of the water column. We collected bottom sediment samples at various locations on the shelf using a 15 L (30 cm$\times$ 30 cm) Van Veer grab. The sediments were analysed in the laboratory to obtain their physical characteristics, such as the particle size distribution and the particle densities. We related the measured OBS to the total suspended solids (TSS) using lab-generated calibration curves determined from the < 63 μm size-fractioned sediments. This size class was chosen because it corresponds to the mean size of the suspended particles estimated by applying the implicit algorithm [10] to the acoustic backscatter measured from the 1 and 4 MHz transducers of the AquaScat profiler.

From the physically-characterized bottom sediments, we estimated the critical shear stress (τ_c) required to initiate sediment motion. We used a relationship, extending the classical Shields expression, that relates the non-dimensional grain diameter D_* to the Shields parameter θ_c [9]:

$$D_* = \left(\frac{Re_*^2}{\theta_c}\right)^{1/3} = d\left(\frac{g(\rho_s-\rho)}{\rho\nu^2}\right)^{1/3} \quad (5)$$

$$\theta_c = \frac{\tau_c}{g(\rho_s-\rho)d} = \frac{0.30}{1+1.2D_*} + 0.055[1-\exp(-0.020D_*)] \quad (6)$$

where g is gravity, ρ_s is the sediment particle density, ρ is the density of water, ν is the kinematic viscosity of water and d is the sediment grain diameter. We use a numerical subscript on τ_c to denote the percentile of the bottom sediments' size distribution used to set d e.g., τ_{c50} implies d was set to the 50th percentile of the particle size distribution.

Results and Discussion

Background forcing

On average during the three-week experiment, the water column was comprised of a well-mixed surface and bottom layer separated by a broad linearly-stratified mid-layer (figure 1). The stratification was weak near the seabed and the depth-averaged buoyancy period was 24 min within the bottom 20 m. The time-averaged velocities measured from the landers' ADCP typically varied between ≈ 0.1 m s^{-1} close to the seabed and increased to 0.2 m s^{-1} at the highest measurement bin (12 m ASB, figure 2). Above 5 m ASB, the principal velocity ellipses were more circular indicating the velocity direction varied more at these heights (figure 2c). In contrast, the principal axes of the depth-averaged velocities show that water flowed generally parallel to the coastline (i.e., north-south) at about 0.2 m s^{-1}, particularly during days 42-46 when the ADVs recorded their peak 10-min time-averaged velocities.

We limit the remainder of our analysis to days 42-46, which includes the period of maximum near-bed velocities (figure 3). Velocities exceeded 0.4 m s^{-1} at 0.4 m ASB, while over the bottom 10 m they peaked at 7 m ASB where the 10-min time-averaged velocities exceeded 0.7 m s^{-1} (figure 3c). This occurred during an 8 h period of prolonged high velocities near the seabed (42.75h figure 3 a,c) that followed the turn of the tide when the 16 °C isotherm suddenly deepened by 80 m (figure 3b). During this period, the depth-averaged velocities reversed briefly northwards with the barotropic tide, while the near-bottom velocities were directed north-east (figure 3d,e). The sediment profiler and the OBS also recorded their highest values of the three-week field experiment during this eight hour period (not shown). The peak TSS estimated from the OBS measurements increased by almost a factor of two at this time, lagging the peak in mean velocities by $\sim$ five hours (figure 3f).

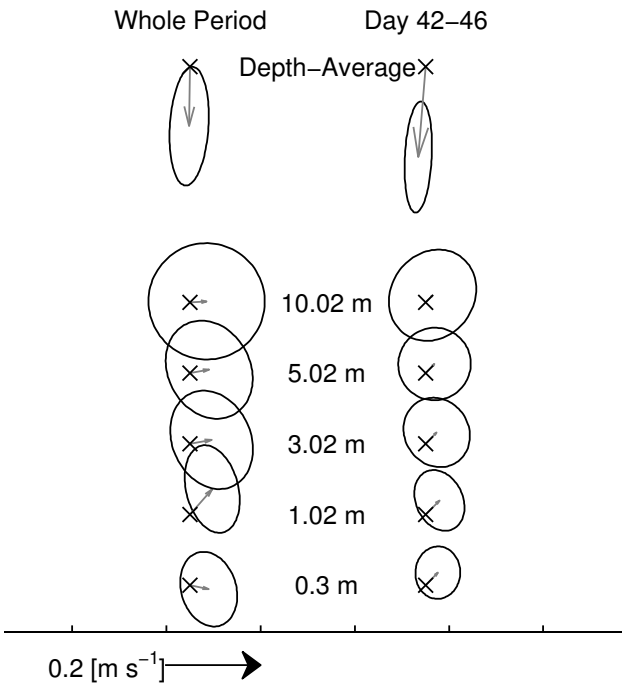

Figure 2: Principal axes determined from the 5-min time-averaged velocities measured over the entire three-week study (left) and over the 4 day period when we measured the sustained high near-bed velocities (right)

Table 2: Summary statistics for τ_w. The correlations R with TSS for the different methods are also included. Correlations and significance (< 0.05) were calculated only from 175 segments that returned τ_w estimates for each method at both heights. We calculated the following critical shear stresses for the bottom sediments: $\tau_{c50} = 0.04$ N m^{-2}, $\tau_{c84} = 0.12$ N m^{-2} and $\tau_{c90} = 0.23$ N m^{-2}.

		TKE		**ID**		**Drag**	
		0.40 m ASB	1.40 m ASB	0.40 m ASB	1.40 m ASB	0.40 m ASB	1.40 m ASB
τ_w [Nm^{-2}]	5th percentile	0.10	0.05	0.02	0.03	0.09	0.09
	Median	0.15	0.13	0.07	0.07	0.17	0.21
	95th percentile	0.38	0.42	0.22	0.52	0.45	0.60
R (p-value)	TSS	0.59 (<0.01)	0.58 (<0.01)	0.42 (0.03)	0.14 (0.49)	0.52 (0.01)	0.50 (0.01)
	Sensor at 0.4 m ASB	-	0.92 (<0.01)	-	0.22 (0.28)	-	0.97 (<0.01)
	ID method	0.50 (0.01)	0.31 (0.12)	-	-	0.37 (0.06)	0.32 (0.11)

Estimated bed shear stress τ_w

Of the three methods for estimating τ_w, the drag method yielded the highest τ_w, followed by the TKE and ID method. The TKE τ_{wT} estimates correlated the most with TSS (table 2), although the τ_w estimates from both the drag and TKE methods appear unrealistically high. The estimates from both methods generally exceeded τ_{c50}, while the median τ_{wD} was of similar magnitude or higher than τ_{c84}. Even during periods when $\tau_{wD} > \tau_{c90}$, sediment did not suspend in the water column given the prolonged periods of low (background) TSS such as $\sim$ day 42-42.5 in figure3f. As noted by [8], C_d can vary by up to an order of magnitude with near bottom flow intensity, but the drag method with the typically used $C_d = 1.5 \times 10^{-3}$ appears to predict unrealistically large bottom stresses.

The ID method provided the lowest and the most reasonable τ_w estimates compared to τ_c. For the ADV nearest to the seabed at 0.4 m ASB, τ_{wI} was almost three times less than τ_{wD} although the median τ_{wI} still exceeded τ_{c50} (table 2). Only the τ_{wI} obtained at 0.4 m ASB correlated significantly with TSS, while those from the TKE and drag method at either height correlated significantly with TSS. Of all three methods, τ_{wI} correlated the least with TSS (table 2). The lack of correlation between TSS and the estimated τ_{wI} at 1.4 m ASB also suggests that this instrument is outside the log-law region near the wall.

Overall, the TKE method appears the most promising predictor for τ_w. In previous studies, this method has yielded the most consistent τ_w estimates between measurement heights, even when the highest measurement is at the outer edge of the log-law region [6]. Laboratory studies around flow deflectors (i.e., where the assumptions of the log-law of the wall are violated), have also shown that the TKE method is a good predictor of sediment suspension [1]. However, the reasons for the unusually large τ_{wT} values compared to τ_c needs further investigation. The universality of the constant of proportionality C_t in equation 4 is debatable [6] and may need to be reduced, while the sediments cohesion may warrant a higher critical shear stress τ_c than predicted via equation 6. In future work, we thus plan to investigate the universality of C_t by estimating turbulence Reynolds stresses and turbulent kinetic energy.

Conclusions

We compared three methods of estimating τ_w against the observed TSS and critical shear stress τ_c required to initiate sediment motion (figure 3f). While the simple drag method correlated best with TSS, the estimated τ_w were excessively high compared to τ_c if we consider the prolonged periods of low (background) TSS when $\tau_{wD} > \tau_{c84}$. In terms of τ_w magnitudes, the "turbulence" methods faired better, in particular the ID method. In the future, we plan to assess the predictions of near-bed shear turbulence stresses τ'_w using the techniques of [7] to predict sediment re-suspension in complex flows.

Acknowledgements

An Australian Research Council Discovery Projects (DP 140101322) and a UWA Collaboration Award funded this work. CEB thanks Aquatec Group for lending an AquaScat sediment profiler as part of their early-career researcher equipment award. We thank the crew aboard the R/V Revelle who aided in the collection of field data and Jessica Hay who analysed the bottom sediment in the laboratory.

References

[1] Biron, P. M., Robson, C., Lapointe, M. F. and Gaskin, S. J., Comparing different methods of bed shear stress estimates in simple and complex flow fields, *Earth Surf. Processes Landforms*, **29**, 2004, 1403–1415.

[2] Bluteau, C. E., Jones, N. L. and Ivey, G. N., Estimating turbulent kinetic energy dissipation using the inertial subrange method in environmental flows, *Limnol. and Oceanogr.: Methods*, **9**, 2011, 302–321.

[3] Boegman, L. and Ivey, G. N., Flow separation and resuspension beneath shoaling nonlinear internal waves, *J. Geophys. Res.*, **114**.

[4] Cacchione, D. A., Pratson, L. F. and Ogston, A. S., The shaping of continental slopes by internal tides, *Science*, **296**, 2002, 724–727.

[5] Diamessis, P. J. and Redekopp, L. G., Numerical investigation of solitary internal wave-induced global instability in shallow water benthic boundary layers, *J. Phys. Oceanogr.*, **36**, 2006, 784–812.

[6] Kim, S.-C., Friedrichs, C. T., Maa, J. P.-Y. and Wright, L. D., Estimating bottom stress in tidal boundary layer from acoustic doppler velocimeter data, *J. Hydraul. Eng.*, **126**, 2000, 399–406.

[7] Mathis, R., Hutchins, N. and Marusic, I., Large-scale amplitude modulation of the small-scale structures in turbulent boundary layers, *J. Fluid Mech.*, **628**, 2009, 311–337.

[8] McGinnis, D. F., Sommer, S., Lorke, A., Glud, R. N. and Linke, P., Quantifying tidally driven benthic oxygen exchange across permeable sediments: An aquatic eddy correlation study, *J. Geophys. Res.–Oceans*, **119**, 2014, 6918–6932.

[9] Soulsby, R. and Whitehouse, R., Threshold of sediment motion in coastal environments, in *Proceedings of the 13th Australasian Coastal and Ocean Engineering Conference and the 6th Australasian Port and Harbour Conference; Volume 1*, University of Canterbury, 1997, 145, 145.

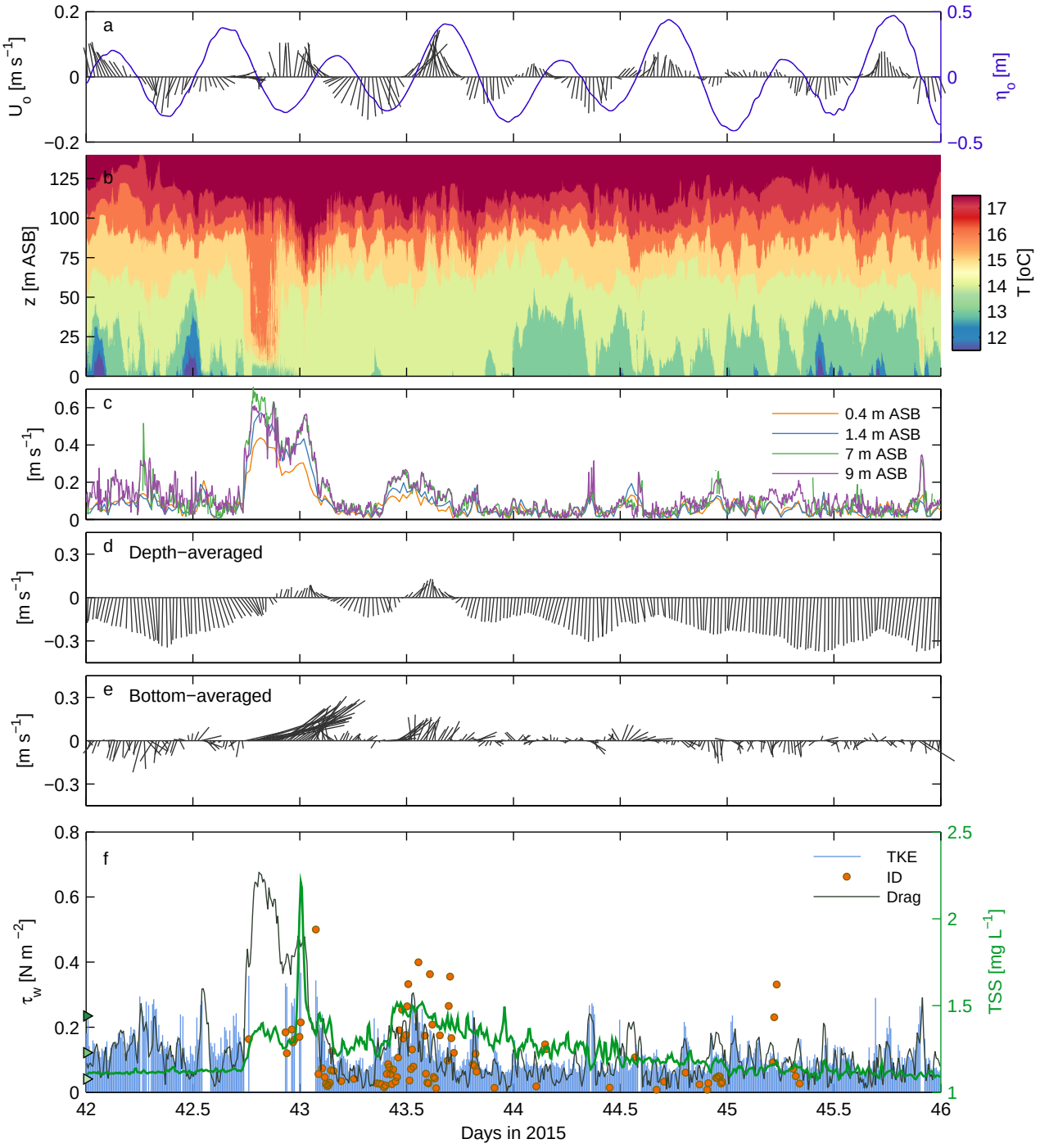

Figure 3: Timeseries of (a) barotropic velocities U_o and elevation η_o; (b) temperature contours; (c) velocity magnitude at discrete heights above the seabed; (d) depth-averaged velocities at the nearby mooring; (e) depth-averaged velocities over the bottom 10 m; (f) estimated τ_w for the different methods at 0.4 m ASB, along with TSS estimated from the OBS measurements on the secondary (green) axis. Panels a, c-e show 10-min time-averaged velocities, while the results in (f) are 512 s averages concurrent with the time segments used to get ε. The green triangles on the left axis of (f) are the critical shear stress τ_c to initiate motion for increasing sediment diameter. These τ_c correspond to the 50th, 84th and 90th percentile diameter obtained from the bottom sediments' particle size distribution.

[10] Thorne, P. D. and Hanes, D. M., A review of acoustic measurement of small-scale sediment processes, *Cont. Shelf Res.*, **22**, 2002, 603–632.

[11] van Rijn, L., *Principles of sediment transport in rivers, estuaries and coastal seas*, number pt. 1 in Principles of Sediment Transport in Rivers, Estuaries, and Coastal Seas, Aqua Publications, 1993.

[12] Venayagamoorthy, S. K. and Fringer, O. B., On the formation and propagation of nonlinear internal boluses across a shelf break, *J. Fluid Mech.*, **577**, 2007, 137–159.